Disturbance rejection for legged robots through a hybrid observer

Viviana Morlando and Fabio Ruggiero

***Abstract*— A legged robot needs to move in unstructured environments continuously subject to disturbances. Existing disturbance observers are not enough when significant forces act on both the center of mass and the robot's legs, and they usually employ indirect measures of the floating base's velocity. This paper presents a solution combining a momentum-based observer for the angular term and an acceleration-based observer for the translational one, employing directly measurable values from the sensors. Due to this combination, we define this observer as "hybrid," and it can detect disturbances acting on both the legged robot's center of mass and its legs. The estimation is employed in a whole-body controller. The framework is tested in simulation on a quadruped robot subject to significant disturbances, and it is compared with existing observer-based techniques.**

I. Introduction

Legged robots can navigate through challenging terrains for tasks such as inspection or search and rescue, thanks to their capabilities of adapting the footstep and overcoming obstacles. Significant advances were made in realizing highly dynamic gaits on real hardware. In particular, biped robots have generated quite an interest, given the inherent instability of their structure. The similitude between a biped and a quadruped robot during highly dynamic gait (*e.g.*, trot, pace, gallop) led to exploit some approaches developed for biped robots to realize quadrupedal locomotion [1], [2].

The most used approach for legged robots combines inverse dynamics and operational-space control. The desired motion is computed for a relevant point of the structure, such as the center of mass (CoM) [3], [4]. Another methodology employs a zero moment point (ZMP) strategy that allows to obtain a modulation of the ground reaction forces adapting the step to the soil during the walking [5], [6]. However, the ability to retain the balance when subject to disturbances remains an open challenge for legged robots in unstructured environments. Different solutions were proposed to reject disturbances during locomotion. Some studies focused on the external wrench of an anticipated touchdown caused by the terrain's irregularity [7], performing an impedance control to obtain a compliant behavior during the impact phase [8].

A widely used approach to cope with external forces is to use an observer. Some disturbance observers were used to detect the anticipated touchdown [9]. In most cases, the observer takes into account only the forces acting on the CoM, and it is integrated into a framework based on the centroidal's dynamics [10], [11], assuming no external forces on swing legs [12], [13]. Using an observer for external wrenches acting only on the CoM robustify the locomotion, but it does not prevent the robot from falling after a severe impact on swing legs. For this reason, a momentum-based observer estimating the disturbances acting on both swing and stance legs was presented in [14]. However, the observer deploys the leg's dynamics, neglecting the CoM's ones. This approximation might be crucial whenever the robot is stressed by major forces acting directly on the CoM.

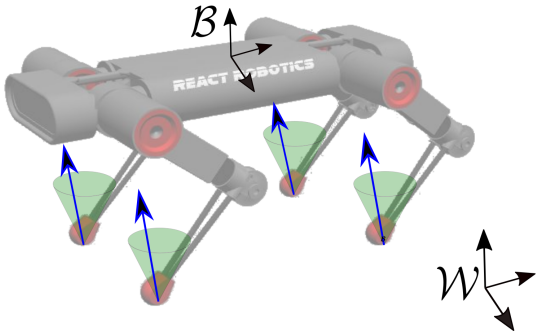

Fig. 1. DogBot, the platform used for simulations. The reference frames for the robot are shown. Ground reaction forces need to stay in the cones.

Usually, a momentum-based observer estimating the external wrench acting on the CoM [11], [10], requires the CoM's translational velocity knowledge. Such a velocity is indirectly obtained through the transformation presented in [15] and not directly from a sensor. An inertial measurement unit (IMU) is typically mounted on moving robots such as legged, aerial, or wheeled ones. This sensor provides the floating base's angular velocity and translational acceleration, leaving the translational velocity to a numerical estimation. For a legged robot, using the centroidal's dynamics, there is the need to (i) compute the floating base's translational velocity and (ii) transform this quantity into the CoM's translational velocity. These computations, alongside the approximation made to obtain the centroidal's dynamics, can bring significant mistakes in estimating the external wrench.

For this reason, this paper proposes a novel estimator, inspired by [16], that comprises three different components. Namely, the first component deals with the CoM's translational part; the second component copes with the CoM's angular part; the third component regards the legs. This last exploit what presented in [14], dealing with disturbances applied to both swing and stance legs. The first and second components are instead designed adopting a *hybrid* observer, that comprises a momentum-based observer for the

The research leading to these results has been supported by the PRINBOT project, in the frame of the PRIN 2017 research program, grant number 20172HHNK5_002.

The authors are with the PRISMA Lab, Department of Engineering and Information Technology, University of Naples Federico II, Via Claudio 21, Naples, 80125, Italy {viviana.morlando, fabio.ruggiero}@unina.it

CoM's angular term and an acceleration-based observer for the translational one, employing directly measurable values from the IMU. Therefore, here, with hybrid, it is intended the combination of two different kinds of observers, the momentum-based and the acceleration-based. Tracking the desired CoM's trajectory is preserved as the rejection of a foot's drift. The control architecture is different from existing approaches, which can guarantee either the CoM's tracking or the drift's rejection only. The observer is integrated into a whole-body controller.

II. Dynamic model and disturbance observer

It is recommended to read [14] as a pre-requisite for a better comprehension of the mathematical part here provided.

A. Model formulation

Legged robots are usually modelled as a free-floating base with some legs attached. Let $\mathcal{B}$ be the frame whose position is attached to the robot's CoM and whose orientation is the one of a fixed frame on the main body, and let $\mathcal{W}$ be the fixed world frame (Fig. 1), respectively. The free-floating base is modelled through 6 virtual joints giving 6 degrees of freedom (DoFs) with respect to $\mathcal{W}$. Moreover, $n_l \geq 2$ legs are attached to the floating base, giving other nn_l DoFs to the structure, with $n > 0$ joints for each leg. Let $x_{com} = \begin{bmatrix} x_c & y_c & z_c \end{bmatrix}^{\mathrm{T}} \in \mathbb{R}^3$, $\dot{x}_{com} \in \mathbb{R}^3$, and $\ddot{x}_{com} \in \mathbb{R}^3$ be the position, velocity, and acceleration of the frame $\mathcal{B}$'s origin with respect to $\mathcal{W}$, respectively. Besides, let $\omega_{com} \in \mathbb{R}^3$ and $\dot{\omega}_{com} \in \mathbb{R}^3$ be the angular velocity and the angular acceleration of $\mathcal{B}$ with respect to $\mathcal{W}$, respectively. The orientation of $\mathcal{B}$ with respect to $\mathcal{W}$ is expressed by the rotation matrix $R_b \in SO(3)$, from which it can be extracted the set of ZYX Euler angles $\phi \in \mathbb{R}^3$. Finally, indicate with $q \in \mathbb{R}^{nn_l}$ the vector collecting the legs' joints. The dynamic model of a legged robot can be formulated in terms of the global CoM through the transformation introduced in [15]. A decoupled structure for the dynamic model is obtained [14], [17], [18] through this transformation, and assuming that the main's body angular motion is slow. Considering that $M_{com,a}$ is the inertia matrix related to the main's body angular motion, through this last assumption, $\frac{d}{dt}\left(M_{com,a}\omega_{com}\right) = M_{com,a}\dot{\omega}_{com}$ holds, meaning that the effect of precession and nutation of the rotating body are discarded [18]. The inertia matrix is $M(q) = \begin{bmatrix} M_{com,l}(q) & O_{3\times 3} & O_{3\times nn_l} \\ O_{3\times 3} & M_{com,a}(q) & O_{3\times nn_l} \\ O_{nn_l\times 3} & O_{nn_l\times 3} & M_q(q) \end{bmatrix} \in \mathbb{R}^{(6+nn_l)\times(6+nn_l)}$; the vector accounting for Coriolis, centripetal, and gravitational forces is $h(q,\upsilon) = \begin{bmatrix} O_{6\times(6+nn_l)} \\ C_q(q,\upsilon) \end{bmatrix}\upsilon + \begin{bmatrix} mg \\ 0_{nn_l} \end{bmatrix}$, with $C_q(q,\upsilon) \in \mathbb{R}^{nn_l\times(6+nn_l)}$, where $\upsilon = \begin{bmatrix} \dot{x}_{com}^{\mathrm{T}} & \omega_{com}^{\mathrm{T}} & \dot{q}^{\mathrm{T}} \end{bmatrix}^{\mathrm{T}} \in \mathbb{R}^{6+nn_l}$ is the stacked velocity; $m > 0$ is the total mass of the robot, $g = \begin{bmatrix} g_0^{\mathrm{T}} & 0_3^{\mathrm{T}} \end{bmatrix}^{\mathrm{T}} \in \mathbb{R}^6$, and $g_0 \in \mathbb{R}^3$ the gravity vector; $0_\times$ and $O_\times$ the zero vector and matrix of proper dimensions. The resultant model is

$$M(q)\dot{\upsilon} + h(q,\upsilon) = S^{\mathrm{T}}\tau + J_{st}(q)^{\mathrm{T}} f_{gr} + J(q)^{\mathrm{T}} f_e + \\ + S_w^{\mathrm{T}} w_{e,c}, \tag{1}$$

with $S = \begin{bmatrix} O_{nn_l\times 6} & I_{nn_l} \end{bmatrix}$ the selection matrix of the actuated part; $\tau \in \mathbb{R}^{nn_l}$ the joint actuation torques; $f_{gr} \in \mathbb{R}^{3n_{st}}$ the ground reaction forces that can be obtained by embedded sensors on robot's feet, with $0 < n_{st} \leq n_l$ the number of stance legs; $f_e \in \mathbb{R}^{3n_l}$ the stacked vector containing the resultant external force at the legs' tips; $S_w = \begin{bmatrix} I_{6\times 6} & O_{6\times nn_l} \end{bmatrix}$ the selection matrix of the un-actuated part; $w_{e,c} = \begin{bmatrix} f_{e,c}^{\mathrm{T}} & \tau_{e,c}^{\mathrm{T}} \end{bmatrix}^{\mathrm{T}} \in \mathbb{R}^6$ the external wrench acting directly on the CoM (it is assumed that the external torques resulting at the legs' tip are negligible); $J_{st}(q) = \begin{bmatrix} J_{st,com}(q) & J_{st,j}(q) \end{bmatrix} \in \mathbb{R}^{3n_{st}\times 6+nn_l}$ and $J(q) = \begin{bmatrix} J_{com}(q) & J_j(q) \end{bmatrix} \in \mathbb{R}^{3n_l\times 6+nn_l}$ Jacobian matrices that are defined in [14]. It can be noticed that the CoM's dynamics are included in the first six rows of (1), decoupled from the legs' dynamics included in the other nn_l rows. It should be noticed that the resultant external forces at the legs' tip, f_e, can be considered as contacts that dictates a net wrench on the CoM, while the wrench directly applied to the CoM, $w_{e,c}$, influences only the CoM's dynamics.

B. Hybrid Observer

Given the decoupled structure of the legged robot's dynamics (1), a hybrid observer is presented, where the forces on the CoM and those on the legs are estimated separately.

1) Estimation for the CoM: Consider the angular centroidal's dynamics composed of the second set of three rows in (1). The generalized angular momentum is expressed as

$$\rho = M_{com,a}\omega_{com}. \tag{2}$$

Then, taking into account (1), the time derivative of (2) is $\dot{\rho} = J_{st,com,a}^{\mathrm{T}} f_{gr} + J_{com,a}^{\mathrm{T}} f_e + \tau_{e,c}$, with $J_{st,com,a} \in \mathbb{R}^{3n_{st}\times 3}$ and $J_{com,a} \in \mathbb{R}^{3n_l\times 3}$ the Jacobians whose transpose map the ground reaction and the external forces into the angular acceleration of the CoM, respectively. Without loss of generality, from (1), define $\tau_c = J_{com,a}^{\mathrm{T}} f_e + \tau_{e,c} \in \mathbb{R}^3$ as the total external torques acting at the CoM, and $\hat{\tau}_c$ as its estimation. The straightforward objective is to achieve $\hat{\tau}_c \simeq \tau_c$. Taking inspiration from [14], the design of the estimator in the time domain is

$$\hat{\tau}_c(t) = K_a\left(\rho(t) - \int_0^t (\hat{\tau}_c(\sigma) + J_{st,com,a}^{\mathrm{T}} f_{gr})\mathrm{d}\sigma\right), \tag{3}$$

where $K_a \in \mathbb{R}^{3\times 3}$ is a positive definite gain matrix. Moreover, it is assumed that $\rho(0) = 0$, meaning that the estimator's kick off should be prior to the robot control. In this case only the angular velocity, available from the IMU, is required. The estimator's dynamics can be written as $\dot{\hat{\tau}}_c + K_a\hat{\tau}_c = K_a\tau_e$, that represents a linear exponentially stable system. To compute the translational component of the wrench acting on the CoM, an acceleration-based observer can be used employing the measurement of the translational

acceleration of the floating base given by the IMU. Considering the linear centroidal's dynamics composed of the first set of three rows in (1), it can be obtained

$$J_{com,l}^{\mathrm{T}} f_e + f_{e,c} = M_{com,l}\ddot{x}_{com} + mg - J_{st,com,l}^{\mathrm{T}} f_{gr}, \quad (4)$$

with $J_{st,com,l} \in \mathbb{R}^{3n_{st}\times 3}$ and $J_{com,l} \in \mathbb{R}^{3n_l\times 3}$ the Jacobians whose transpose map the ground reaction and the external forces into the linear acceleration of the CoM, respectively. From (1), consider $f_c = J_{com,l}^{\mathrm{T}} f_e + f_{e,c} \in \mathbb{R}^3$ as the current total external force at the CoM, and $\hat{f}_c \in \mathbb{R}^3$ as the estimated one. The following first-order stable filter can be applied

$$\hat{f}_c(t) = K_l \int_0^t (M_{com,l}\ddot{x}_{com} + mg - J_{st,com,l}^{\mathrm{T}} f_{gr} - \hat{f}_c)\mathrm{d}\sigma \quad (5)$$

to obtain the estimator's dynamics $\dot{\hat{f}}_c + K_l \hat{f}_c = K_l f_c$, where $K_l \in \mathbb{R}^{3\times 3}$ is a positive definite gain matrix.

2) Estimation for the legs: For the disturbances acting on the legs, the momentum-based observer presented in [14] is employed, based on the last nn_l rows of (1). Consider $f_j = J_j^{\mathrm{T}} f_e \in \mathbb{R}^{nn_l}$ as the effect at the joint torques of the resultant force at the legs' tips, and $\hat{f}_j \in \mathbb{R}^{nn_l}$ as its estimation, respectively. The chosen second-order estimator can be written as $\hat{f}_j(t) = K_{2,j}\int_0^t(-\hat{f}_j(\sigma) + K_{1,j}\left(\rho_j(t) - \int_0^t(\hat{f}_j(\sigma) + C_q^{\mathrm{T}}\dot{q} + \tau + J_{st,j}^T f_{gr})\mathrm{d}\sigma\right))\mathrm{d}\sigma$, with $K_{1,j}, K_{2,j} \in \mathbb{R}^{(nn_l)\times(nn_l)}$ positive definite gain matrices. Further details related to this observer can be found in [14]. Recalling the external forces at the legs' tips f_e, its estimation $\hat{f}_e \in \mathbb{R}^{3n_l}$ can be retrieved through

$$\hat{f}_e = J_j^{T^\dagger}\hat{f}_j \quad (6)$$

Then, the full observer is composed by (3), (5), and (6).

III. Whole-body Controller

The estimator presented above, a motion planner, and an optimization problem shape the designed controller.

A. Motion planning

The motion is continuously replanned so that the ZMP is always maintained inside the support polygon [5]. From now on, the position and the orientation of the frame $\mathcal{B}$ will be stacked into $r_c = \begin{bmatrix} x_{com}^{\mathrm{T}} & \phi^{\mathrm{T}}\end{bmatrix}^{\mathrm{T}} \in \mathbb{R}^6$, while its velocity and acceleration can be considered $\upsilon = \begin{bmatrix}\dot{x}_{com}^{\mathrm{T}} & \omega_{com}^{\mathrm{T}}\end{bmatrix}^{\mathrm{T}} \in \mathbb{R}^6$ and $\dot{\upsilon}_c = \begin{bmatrix}\ddot{x}_{com}^{\mathrm{T}} & \dot{\omega}_{com}^{\mathrm{T}}\end{bmatrix}^{\mathrm{T}} \in \mathbb{R}^6$. For each footstep, the motion is split into two phases, replanning the desired trajectory for the CoM at the beginning of each footstep, with a period $T_{fs} > 0$. The motion planner computes the reference $r_{c,ref}$, $\dot{\upsilon}_{c,ref}$ and $\ddot{\upsilon}_{c,ref} \in \mathbb{R}^6$ for the CoM and the reference $x_{sw,des} \in \mathbb{R}^{3(n_l - n_{st})}$ for the swing feet as a $3-$rd order splines. Further details in [14].

B. Quadratic problem

The wrench-based optimization problem used in this paper is based on [14] with suitable modifications to include the hybrid estimator. Let $\zeta = \begin{bmatrix}\dot{\upsilon}_c^{\mathrm{T}} & \ddot{q}^{\mathrm{T}} & f_{gr}^{\mathrm{T}}\end{bmatrix}^{\mathrm{T}} \in \mathbb{R}^{6+nn_l+3n_{st}}$ be the chosen control variables. The addressed problem is

$$\underset{\zeta}{\text{minimize}} \quad f(\zeta) \quad (7)$$

$$\text{subject to} \quad A\zeta = b, \quad (8)$$

$$D\zeta \leq c. \quad (9)$$

Each term of the problem is detailed in the following.

1) Cost function: The cost function tracks the CoM's reference coming from the motion planner, reducing as much as possible the control effort. To this aim, the desired wrench at the robot's CoM is computed using the first six equations of (1) and the references from the motion planner, as $w_{com,des} = K_p(r_{c,ref} - r_c) + K_d(\upsilon_{c,ref} - \upsilon_c) + mg + M_{com}(q)\dot{\upsilon}_{c,ref}$, with $K_p, K_d \in \mathbb{R}^{6\times 6}$ positive definite matrices. Let $\hat{w}_{com} = \begin{bmatrix}\hat{f}_c^{\mathrm{T}} & \hat{\tau}_c^{\mathrm{T}}\end{bmatrix}^{\mathrm{T}}$ be the estimated external wrench at the CoM, the cost function minimizing the desired wrench and compensating for the disturbance can be written as $f(\zeta) = \left\|J_{st,com}^{\mathrm{T}}\Sigma\zeta - (w_{com,des} - \hat{w}_{com})\right\|_Q + \left\|\zeta\right\|_R$, with $\Sigma \in \mathbb{R}^{3n_{st}\times(6+nn_l+3n_{st})}$ a matrix selecting the last $3n_{st}$ elements of ζ, $Q \in \mathbb{R}^{6\times 6}$ and $R \in \mathbb{R}^{(6+nn_l+3n_{st})\times(6+nn_l+3n_{st})}$ two symmetric and positive definite matrices that can be used to specify the relative weight between the components of the cost function, and $\|\cdot\|_\times$ the quadratic form with proper matrix.

2) Equality constraints: Two equality constraints need to be imposed. The first one regards the dynamic consistency, employing the first six rows of (1) as follows

$$\begin{bmatrix} M_{com}(q) & 0_{6\times nn_l} & -J_{st,com}(q)^T\end{bmatrix}\zeta = -mg. \quad (10)$$

The second equality constraint maintains the contact of the stance feet imposing their velocity equal to zero as $J_{st}(q)\upsilon = 0_{3n_{st}}$, whose time derivative is

$$\begin{bmatrix} J_{st,com} & J_{st,j} & O_{3n_{st}\times 3n_{st}}\end{bmatrix}\zeta = -\dot{J}_{st,com}\upsilon_c - \dot{J}_{st,j}\dot{q}. \quad (11)$$

3) Inequality constraints: To avoid slipping, ground reaction forces need to be constrained inside a friction cone (Fig. 1), approximated as a pyramid to obtain linear constraints in the problem. Considering the i-th ground reaction force $f_{gr,i} \in \mathbb{R}^3$, with $i = 1, \ldots, n_{st}$, and indicating with $\bar{n}_i \in \mathbb{R}^3$ the i-th normal vector, $\bar{l}_{1,i}, \bar{l}_{2,i} \in \mathbb{R}^3$ two tangential vectors related to the i-th contact with the ground, $\mu > 0$ the friction coefficient, the constraints can be written as [19]

$$\begin{aligned}(\bar{l}_{1,i} - \mu\bar{n}_i)^T f_{gr,i} \leq 0, \quad -(\bar{l}_{1,i} + \mu\bar{n}_i)^T f_{gr,i} \leq 0,\\ (\bar{l}_{2,i} - \mu\bar{n}_i)^T f_{gr,i} \leq 0, \quad -(\bar{l}_{2,i} + \mu\bar{n}_i)^T f_{gr,i} \leq 0.\end{aligned} \quad (12)$$

For mechanical and safety reasons, constraints to limit the joint torques need to be imposed. Being $\tau_{min}, \tau_{max} \in \mathbb{R}^{nn_l}$ the minimum and maximum torques, considering the last nn_l rows of (1), the constraints can be expressed as

$$\begin{aligned}\tau_{min} - C_q(q,v)\dot{q} \leq \begin{bmatrix} O_{nn_l\times 6} & M_q(q) & -J_{st,j}(q)^T\end{bmatrix}\zeta\\ \leq \tau_{max} - C_q(q,v)\dot{q}.\end{aligned} \quad (13)$$

The last constraint allows the robot to follow the trajectory planned for the swing feet. This constraint exploits the

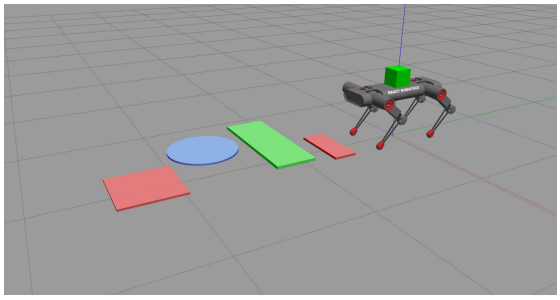

Fig. 2. Scenario used for Case Study 1.

estimation of external forces from (6) acting on swing legs $\hat{f}_{e,sw} \in \mathbb{R}^{3(n_l-n_{st})}$. These disturbances can heavily affect the respective foot's motion, causing a drift. To compensate for them, operational space formulation for swing feet is employed, using the following command acceleration

$$\ddot{x}_{sw,c} = \ddot{x}_{sw,d} + K_{d,sw}(\dot{x}_{sw,d} - \dot{x}_{sw}) + \\ + K_{p,sw}(x_{sw,d} - x_{sw}) - J_{sw}M_c^{-1}PJ_{sw}^T\hat{f}_{e,sw} \tag{14}$$

with $M_c = PM + I_{6+nn_l} - P$ and $P \in \mathbb{R}^{6+nn_l \times 6+nn_l}$ an orthogonal projection operator [14]. This constraint is softened by adding slack variables $\gamma \in \mathbb{R}^{3(n_l-n_{st})}$ within the problem. The addressed inequality constraint is [14]

$$\ddot{x}_{sw,c} - \gamma - \dot{J}_{sw}\upsilon \leq \begin{bmatrix} J_{sw,com} & J_{sw,j} & O_{3(n_l-n_{st})\times 3n_{st}} \end{bmatrix} \zeta \leq \\ \ddot{x}_{sw,c} + \gamma - \dot{J}_{sw}\upsilon. \tag{15}$$

4) Control torques: Given the result of the optimization problem, the control torques can be computed using the last nn_l rows of (1) as $\tau = M_q(q)\ddot{q} + C_q(q,v)\dot{q} - J_{st,j}(q)^T f_{gr}$, considering that all the external forces have been compensated for inside the quadratic problem.

IV. Case Studies

A. Setup

Simulations have been carried out through the ROS middleware, in combination with the dynamic simulator *Gazebo*. This choice has been made since Gazebo uses a high-performance physics engine to make the movement and external conditions as realistic as possible. The quadruped used for simulations in Gazebo is DogBot from React Robotics, an open-source platform whose structure is shown in Fig. 1. Details about the quadruped's structure can be found in [14]. Force sensors have been added to the robot's feet to obtain ground reaction forces, the effect of their measures' error on the observer on the legs have been studied in [14] All the simulations were performed on a standard personal computer. The stance phase has been chosen to last 0.15 s, while the swing phase lasts 0.115 s. Numerical integration for dynamics is set in Gazebo as $\delta\ t = 0.001$ s. The torque control loop, the state estimation, and the momentum-based observation have a frequency of 1 kHz, while the optimization problem runs at a frequency of 400 Hz. In order to test the whole-body control design, three case studies

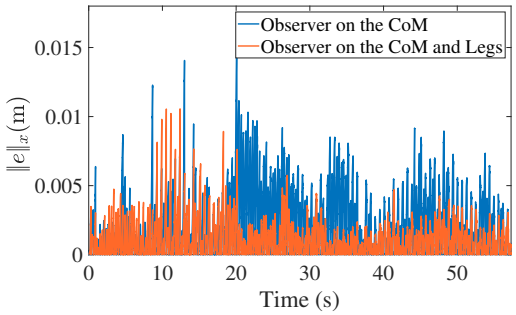

(a)

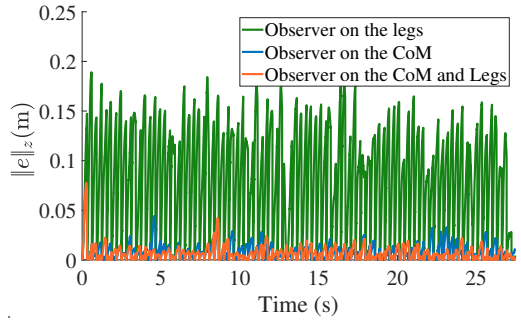

(b)

Fig. 3. Case Study 1. Error on the $x-$axis (a) and on the $z-$axis (b).

are considered in the following. The case studies can be appreciated in the video[1], while the code is also available[2].

B. Case study 1

This case study aims to test the controller in a realistic scenario, presented in Fig. 2, where some blocks with different heights and friction coefficients have been added to reproduce an irregular terrain. With reference to Fig. 2, the heights of the blocks are 0.015 m for the blue blocks, 0.035 m for the green ones, and 0.02 m for red blocks. Instead, in Gazebo, the friction coefficients between the legs and the blocks are set to 0.4, 0.6, 0.8, respectively, while 1 is the friction coefficient with the ground. To test robustness, the friction coefficient inside the whole-body controller has been chosen, in a conservative way, as 0.4. An object of 23 kg has been put on the robot's torso for further stress. It should be noticed that the objective of this case study is not the object transportation but to test the capability of the controller to handle such a disturbance. Combining an irregular terrain with an object on the torso is a suitable scenario for testing disturbances on both the CoM and the legs. Here, the forward direction is along the $x-$axis, with a velocity of 0.12 m/s. The controller here presented (CoM and legs) is compared with the one in [14], which uses only the estimation on the legs, and the controller employing only the estimation on the CoM [20], thus without the compensation of disturbances on swing legs implemented in (14). The results showed that this kind of stress is difficult to handle using only the estimation on the legs. Indeed, it

[1] https://youtu.be/wbtoAo3Y6Xc
[2] https://github.com/prisma-lab/WBC-quadruped-DOB

can be seen in Fig. 3b that the error along the $z-$axis is one order of magnitude higher than the error obtained when the observation on the CoM is present. This is plausible since the object impresses a significant disturbance on the CoM that cannot be seen through the legs' observer, making the robot lower its torso and fall. Comparing the two controllers addressing the estimation on the CoM, their errors on the $z-$axis are similar, while on the $x-$axis the presented hybrid estimator has better performances. This happens because the presence of irregular terrains causes anticipated touchdowns that can be better handled using observation on the legs. Irregular terrain may thus unbalance the robot if it only uses an observer on the CoM. The estimation of the wrench at the CoM is reported in Fig. 4b. It can be seen that the most critical estimation regards the force acting along the $z-$axis, whose mean is -228.0635 N. This is given by the object's weight, which, given the gravity acceleration, imposes a force of around -225.6300 N. The estimation demonstrates to be valid enough to handle this force retaining the balance.

C. Case study 2

The second case study has been carried out considering two random disturbances: the first acting on the CoM and the second acting on a randomly chosen point of one of the legs. Every four seconds, the force's magnitude changes randomly between 2.5 N and 40 N. The direction of the disturbance forces is shown in the multimedia attachment. The forward direction is along the $y-$axis, with a velocity of 0.12 m/s. Furthermore, this case study has been tested in a non-ideal situation by adding a white Gaussian noise on the joint torque and the ground reaction forces measurements, emulating sensors noise. The chosen standard deviation is 10% of the measured signal. This case study aims to demonstrate the validity of the proposed hybrid observer, acting on both the CoM and the legs. The observer only on the CoM seems unable to reject the disturbance acting on the legs, with a significant drift of the foot that causes the fall. Further case studies demonstrating the failure of this observer in similar situations can be found in [14]. Instead, the observer only on the legs seems to guarantee a good tracking of the planned foothold. However, it cannot reject the disturbance on the CoM with a consequent fall. Finally, using the presented hybrid estimator, the robot can reject the disturbance on the CoM and have good tracking of the planned foothold at the same time. The approach results robust, with a maximum error in the tracking of the CoM of 0.02 m, shown in Fig. 5. The estimation of the magnitude acting on the CoM and the rear right leg are presented in Figs. 6 and 7. In this way, good tracking of the actual disturbances can be observed.

D. Case Study 3

This case study considers random disturbances as in the previous one plus a parametric uncertainty of the total mass known by the controller, changed by 30%. Besides, the blocks already employed in case 1 are used to simulate an irregular terrain. The capabilities of the controller are now tested in a complex situation with (i) high external forces

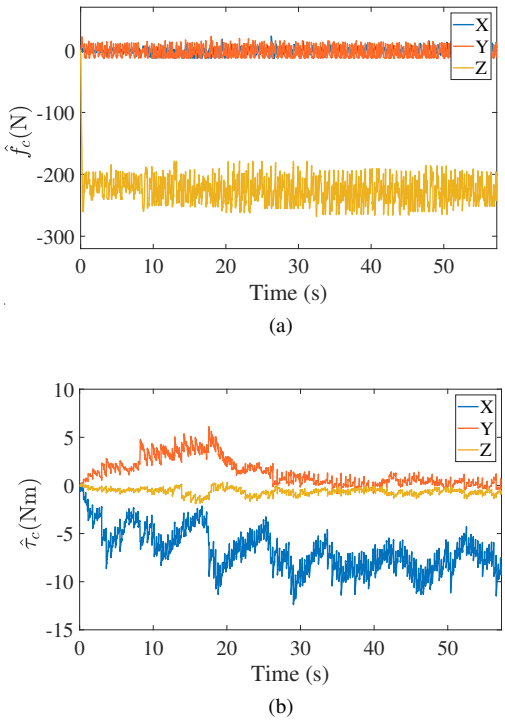

Fig. 4. Case Study 1. Estimation of $\hat{f}_c$ (a) and $\hat{\tau}_c$ (b).

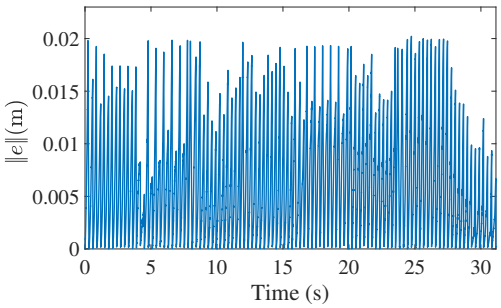

Fig. 5. Case Study 2. Error norm of the robot's CoM using the proposed controller.

stressing the robot and simulating impact with objects or pushes; (ii) a rough terrain; (iii) parametric uncertainties.

From Fig. 8, the peaks of CoM's error norm are higher but always less than 0.025 m. However, this small error increment may be caused by the parametric uncertainty and the irregular terrain, which can still be handled anyway.

V. Conclusion

This paper presented a hybrid observer for a legged system, acting both at the robot's CoM and its legs. In contrast with the existing literature, the well-established momentum-based and acceleration-based observers were combined to use only the measures directly available from sensors. Then, the devised observer was integrated into a whole-body controller, compensating for external forces acting on the CoM, stance, and swing legs. The proposed approach was tested in a realistic simulation environment through three case studies. The controller allows the locomotion of a legged robot inside a complex environment, where collisions could happen, but also in case of parametric uncertainties.

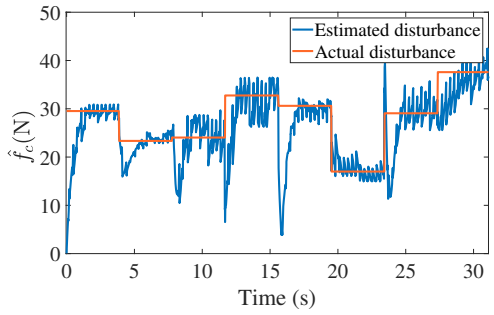

(a)

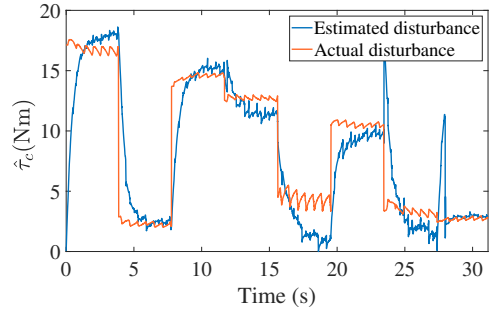

(b)

Fig. 6. Case Study 2. Estimation of $\hat{f}_c$ (a) and $\hat{\tau}_c$ (b).

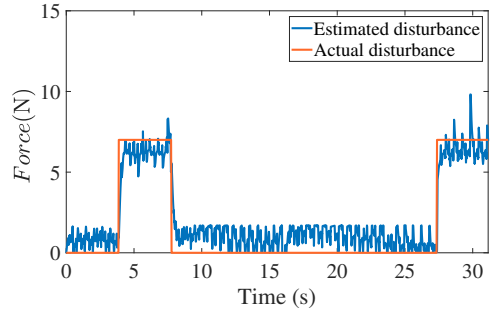

Fig. 7. Case Study 2. Estimation of $\hat{f}_e$ for the rear right leg.

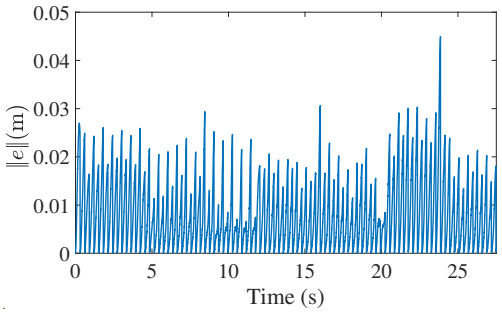

Fig. 8. Case Study 3. Error norm of the robot's CoM using the proposed controller.

REFERENCES

[1] N. Dini and V. J. Majd, "An MPC-based two-dimensional push recovery of a quadruped robot in trotting gait using its reduced virtual model," *Mechanism and Machine Theory*, vol. 146, 2020.

[2] A. W. Winkler, F. Farshidian, M. Neunert, D. Pardo, and J. Buchli, "Online walking motion and foothold optimization for quadruped locomotion," in *2017 IEEE International Conference on Robotics and Automation*, 2017, pp. 5308–5313.

[3] O. E. Ramos, N. Mansard, and P. Soueres, "Whole-body motion integrating the capture point in the operational space inverse dynamics control," in *2014 IEEE International Conference on Humanoid Robots*, 2014, pp. 707–712.

[4] G. Xin, H.-C. Lin, J. Smith, O. Cebe, and M. Mistry, "A model-based hierarchical controller for legged systems subject to external disturbances," in *2018 IEEE International Conference on Robotics and Automation*, 2018, pp. 4375–4382.

[5] C. D. Bellicoso, F. Jenelten, P. Fankhauser, C. Gehring, J. Hwangbo, and M. Hutter, "Dynamic locomotion and whole-body control for quadrupedal robots," in *2017 IEEE/RSJ International Conference on Intelligent Robots and Systems*, 2017, pp. 3359–3365.

[6] C. D. Bellicoso, F. Jenelten, C. Gehring, and M. Hutter, "Dynamic locomotion through online nonlinear motion optimization for quadrupedal robots," *IEEE Robotics and Automation Letters*, vol. 3, no. 3, pp. 2261–2268, 2018.

[7] Q. Bombled and O. Verlinden, "Indirect foot force measurement for obstacle detection in legged locomotion," *Mechanism and Machine Theory*, vol. 57, pp. 40–50, 2012.

[8] M. A. Hopkins, D. W. Hong, and A. Leonessa, "Compliant locomotion using whole-body control and divergent component of motion tracking," in *2015 IEEE International Conference on Robotics and Automation*, 2015, pp. 5726–5733.

[9] G. Bledt, P. M. Wensing, S. Ingersoll, and S. Kim, "Contact model fusion for event-based locomotion in unstructured terrains," in *2018 IEEE International Conference on Robotics and Automation*, 2018, pp. 4399–4406.

[10] J. Englsberger, G. Mesesan, and C. Ott, "Smooth trajectory generation and push-recovery based on divergent component of motion," in *2017 IEEE/RSJ International Conference on Intelligent Robots and Systems*, 2017, pp. 4560–4567.

[11] M. Focchi, R. Orsolino, M. Camurri, V. Barasuol, C. Mastalli, D. G. Caldwell, and C. Semini, "Heuristic planning for rough terrain locomotion in presence of external disturbances and variable perception quality," in *Advances in Robotics Research: From Lab to Market*, 2020, pp. 165–209.

[12] N. Dini, V. J. Majd, F. Edrisi, and M. Attar, "Estimation of external forces acting on the legs of a quadruped robot using two nonlinear disturbance observers," in *2016 4th International Conference on Robotics and Mechatronics*, 2016, pp. 72–77.

[13] N. Dini and V. J. Majd, "Sliding-mode tracking control of a walking quadruped robot with a push recovery algorithm using a nonlinear disturbance observer as a virtual force sensor," *Iranian Journal of Science and Technology, Transactions of Electrical Engineering*, pp. 1–25, 2019.

[14] V. Morlando, A. Teimoorzadeh, and F. Ruggiero, "Whole-body control with disturbance rejection through a momentum-based observer for quadruped robots," *Mechanism and Machine Theory*, vol. 164, p. 104412, 2021.

[15] C. Ott, M. A. Roa, and G. Hirzinger, "Posture and balance control for biped robots based on contact force optimization," in *2011 11th IEEE-RAS International Conference on Humanoid Robots*, 2011, pp. 26–33.

[16] T. Tomić, C. Ott, and S. Haddadin, "External wrench estimation, collision detection, and reflex reaction for flying robots," *IEEE Transactions on Robotics*, vol. 33, no. 6, pp. 1467–1482, 2017.

[17] B. Henze, C. Ott, and M. Roa, "Posture and balance control for humanoid robots in multi-contact scenarios based on model predictive control," in *2014 IEEE/RSJ International Conference on Intelligent Robots and Systems*, 2014, pp. 3253–3258.

[18] J. Di Carlo, P. M. Wensing, B. Katz, G. Bledt, and S. Kim, "Dynamic locomotion in the mit cheetah 3 through convex model-predictive control," in *2018 IEEE/RSJ International Conference on Intelligent Robots and Systems*, 2018, pp. 1–9.

[19] C. D. Bellicoso, C. Gehring, J. Hwangbo, P. Fankhauser, and M. Hutter, "Perception-less terrain adaptation through whole body control and hierarchical optimization," in *2016 IEEE-RAS 16th International Conference on Humanoid Robots*, 2016, pp. 558–564.

[20] S. Fahmi, C. Mastalli, M. Focchi, and C. Semini, "Passive whole-body control for quadruped robots: Experimental validation over challenging terrain," *IEEE Robotics and Automation Letters*, vol. 4, no. 3, pp. 2553–2560, 2019.